Available online at www.sciencedirect.com

ScienceDirect

Procedia Structural Integrity 38 (2022) 564–571

Structural Integrity Procedia

www.elsevier.com/locate/procedia

FATIGUE DESIGN 2021, 9th Edition of the International Conference on Fatigue Design

Investigation of residual stresses and microstructure effects on the fatigue behaviour of a L-PBF AlSi10Mg alloy

Ilaria Roveda[a,]*, Itziar Serrano-Munoz[a], Arne Kromm[a], Mauro Madia[a]

[a]*Bundesanstalt für Materialforschung und -prüfung, Unter den Eichen 87, 12205 Berlin*

Abstract

Al-Si alloys produced by Laser Powder Bed Fusion (L-PBF) techniques allow the fabrication of lightweight free-shape components that find space in aerospace, automotive, biomedical and military applications. Due to the high cooling rates occurring during the building process, L-PBF AlSi10Mg alloys exhibit an ultra-fine microstructure that leads to superior mechanical properties in the as-built condition compared to conventional cast Al-Si materials. Nevertheless, L-PBF processing induces high thermal gradients, leading to deleterious residual stress levels that must be considered to avoid part distortion and unpredicted failures. In order to relax detrimental residual stress and to increase the ductility, post-processing stress relief treatments are generally performed. In as-built condition the hypoeutectic AlSi10Mg microstructure consist of fine α-Al cells containing uniformly dispersed silicon nanoparticles, which are, in addition, surrounded by a eutectic Si network. Above 260°C the silicon interconnectivity starts to breakdown into spheroidized particles and to coarsen. At the same time, the heating residual stresses are relieved.

The objective of the contribution is to investigate, under different heat treatment conditions, the evolution of microstructure and residual stresses in view of optimizing the fatigue performance of the alloy. To this purpose various heat treatments in a range of temperatures between 265°C and 300°C for a duration between 15 minutes and 2 hours are performed. The microstructure modifications are analysed using a scanning electron microscope and the residual stress state is measured by laboratory X-ray diffraction.

Keywords: AlSi10Mg alloy; additive manufacturing; L-PBF; residual stress; heat treatment

* Corresponding author. Tel.: +49 30 8104-3189; fax: +49 30 8104-73189.
E-mail address: ilaria.roveda@bam.de

10.1016/j.prostr.2022.03.057

1. Introduction and state-of-the-art

Additive manufacturing (AM) technologies are reaching a well-established position in the production of high-performance components. Nevertheless, as the technique is still relatively new and considering the complexity of the topic, further investigations are even now required.

Among the available techniques, Laser Powder Bed Fusion (L-PBF) processes allow the fabrication of metallic components layer-by-layer, reducing the amount of post-processing needed. Typically, a near complex net-shape component can be produced, minimizing the waste of raw material as well as the use of expensive subtractive tools.

The L-PBF technique is particularly interesting for lightweight alloys as it offers advantages over the well-established casting processes. L-PBF AlSi10Mg materials possess, in the as-built condition, increased mechanical properties compared to the traditionally casting Al-Si due to the formation of finer nano-silicon networks and smaller grains. These microstructural features result from localized rapid cooling rates occurring during the process (Thijs et al. (2013)).

The high thermal gradients occurring during the process also induce the build-up of high residual stress (RS). To avoid unexpected failures as a result of unaccounted RS, as well as to increase the ductility of the material, post-processing heat treatments are commonly applied before the component is placed on the market and put into service.

From the current literature, a lack of knowledge on the influence of the microstructure and the residual stresses on the fatigue performances has emerged. RS can be detrimental or beneficial for the fatigue life of a component depending on their sign (tensile or compressive, respectively). Even though a large body of research has been conducted on other L-PBF materials such as TiAl6V4 and IN718, the topic remains mainly unexplored in L-PBF Al-Si materials.

Traditionally, the post-process heat treatment most studied in literature (Wang et al. (2018), Takata et al. (2017), Zhou et al. (2018)) and applied by the industry is the T6. A T6 heat treatment consists of a first solution heat treatment at high temperature (greater than 500°C) for 1-5 hours, followed by an ageing step at temperatures between 100°C and 180°C for 10-12 hours. Solutionizing above 500°C enables the homogenization of the microstructure and a complete relief of the residual stresses is expected. However, the fine microstructure with interconnected eutectic-Silicon is broken down into coarse particles and the formation of deleterious needle-like β iron intermetallics occurs, which leads to a reduction in strength.

Beside these high temperature heat treatments, low temperature stress-relief heat treatments (typically at 300°C) are finding place in the latest publications. At these temperatures, the overgrowth of silicon particles is avoided. In this context, there is ample window for further research.

The response of the material to heating can be investigated by Differential Scanning Calorimetry (DSC). DSC analysis can highlight the temperatures at which modifications in the microstructure occur. In the studies by (Yang et al. (2018), Fiocchi et al. (2021) and Marola et al. (2018)), two exothermic peaks are observed for the L-PBF alloy: peak A, lying at approximately 260 °C, and peak B at 320 °C. The thermographs were recorded with a constant heating rate of 20°C/min. In this way, microstructural evolution occurs while the temperature is increasing. For this reason, these temperatures need to be adapted in case of heat treatments, where a certain temperature is reached and kept for a certain time (soaking time): in case of isothermal heat treatments the peaks can be observed at 265°C and 295°C (Fiocchi et al. (2016)).

Different authors interpretated the cause of these peaks yielding different conclusions. In summary, peak A should be attributed to Si precipitation from the supersaturated matrix and peak B to the superposition of two effects: formation of the Mg_2Si phase and Si diffusion along the eutectic network.

More in detail, during heating the microstructure undergoes the following evolution, which is well summarised by Fiocchi et al. (2021). A simplified scheme is shown in Figure 1 for easier understanding.

At room temperature, in the as-built state, the Si atoms are dissolved in the aluminium supersaturated matrix (white cells in Figure 1a), surrounded by eutectic Si-networks (in black in Figure 1a). Increasing the temperature, the first modification occurs above 265°C, where Si atoms are rejected from the matrix and precipitate along the pre-existing cellular boundaries (Figure 1b). Thereafter, at 295°C the fragmentation and spheroidization of the Si branches takes place, presumably by Al–Si interdiffusion (Figure 1c). The original eutectic fine fibrous network is completely removed and replaced by uniformly distributed blocky particles. Above 400°C the Si particles are coarsened and iron needle-shaped β intermetallics are formed (Figure 1d).

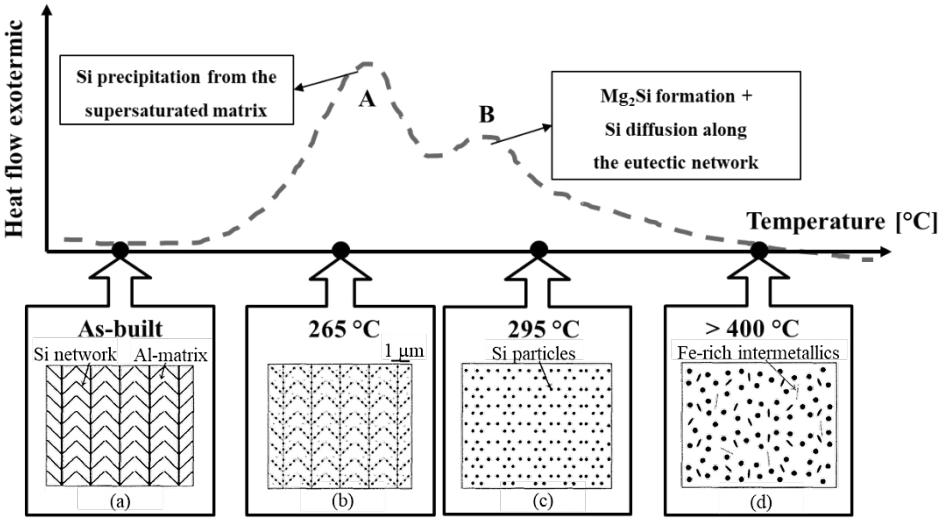

Figure 1: Schematic description of the modifications in the microstructure occurring during heating, see Li et al. (2016) and Fiocchi et al. (2016).

In the current study, the evolution of microstructure and RS is investigated after different stress relief heat treatments. Specifically, a heat treatment at 265°C for 1 hour and four heat treatments of different duration at 300°C were performed. Therefore, changes in the silicon morphology during the soaking stage at 300°C were investigated more in detail after 15 min, 30 min, 1 h and 2h.

2. Material and methodology

2.1. L-PBF-AlSi10Mg samples production

The samples were produced under argon atmosphere through a Concept Laser M2 machine by the Deutsche Zentrum für Luft- und Raumfahrt (DLR). Cylindric samples with a diameter of 12 mm and a height of 134 mm were manufactured. The height of the samples is parallel to the building direction (BD). The scan strategy adopted consists of 5x5 mm^2 squares with 45° rotating scan vectors, as shown in Figure 2.

The building platform during the process has been kept at a temperature of 200°C to reduce thermal stress and part distortion (Buchbinder et al. (2014)).

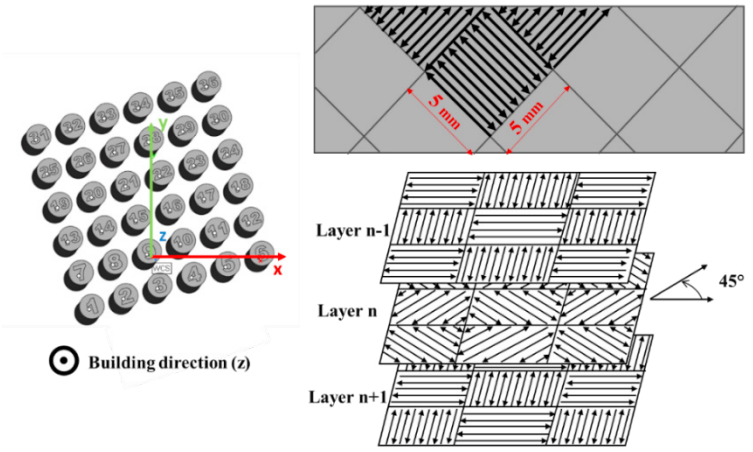

Figure 2: Scan strategy adopted during the L-PBF process. Position of the cylindrical and prismatic samples on the base plate and laser path.

The manufacturing parameters are reported in Table 1.

Table 1: L-PBF process parameters

L-PBF machine	Power, [W]	Hatch space, [mm]	Velocity, [mm/s]	Layer thickness, [mm]	Temperature building platform, [°C]	Atmosphere
Concept Laser M5	380	0,1	1500	0.03	200	Argon

2.2. Microscopy

The evolution of the microstructure after heat treatments was investigated using a Scanning Electron Microscope (SEM). The metallographic samples are extracted from the central part of the cylindric specimens illustrated in Figure 2. The samples were etched to enhance the contrast between the aluminium matrix and the eutectic silicon with a Dix & Keller solution (mixture reported in Table 2).

Table 2: Dix & Keller reagent used to prepare the AlSi10Mg samples before microscopy.

Dix & Keller:	
190 ml	H_2O
5 ml	HNO_3
10 ml	HCl
2 ml	HF

2.3. Non-destructive testing

The residual stresses were measured along the height of small cylindric samples with a height of 60 mm (for the heat treated samples) and 65 mm (for the as-built sample). These specimens were obtained by cutting the initially fabricated samples in half. X-Ray diffraction with CrKα radiation using a 1 mm collimator was performed to determine the RS on the Al{311} lattice plane. The penetration depth of about 10 µm allowed the use of the $\sin^2\psi$-method assuming a biaxial stress state in the surface. With the help of a laboratory diffractometer setup 21 tilts in the ψ angle range from -45° to +45° were applied. For the calculation of stresses, the following elastic constants were used:

- Young's modulus E = 70 600 MPa
- Poisson's ratio υ = 0.345.

3. Results

The literature review of the state-of-the-art introduced in Section 1 guided the selection of the most promising temperatures and durations to be used as stress relief heat treatments.

The chosen heat treatments (performed using small samples, see Table 3) were carried out at BAM using a PEO-630 Furnace with pressurized air and a heating and cooling rate of 10°C/min.

Table 3: Heat treatments performed at BAM.

Heat treatment	Temperature [°C]	Duration [min]
1) Stress relief	265	60
2) Stress relief	300	15
3) Stress relief	300	30
4) Stress relief	300	60
5) Stress relief	300	120

The as-built state (Figure 3a) shows a thin nanometric Si-rich network, which is mostly interconnected and encloses the α-Al matrix. The aluminium cells contain very fine precipitates with a diameter generally smaller than 20 nm. After a stress relief heat treatment at 265°C (Figure 3b), the microstructure remains mainly unaltered. However, the Si network becomes thicker. This could be related to the silicon that is rejected from the supersaturated aluminium matrix and precipitates along the boundaries. At 300°C, the Si network is broken down and transformed into Si particles (Figure 3c). These particles show a wide size range. The large size variation can be associated with the fact that the big particles are globularized from the initial Si-rich network and the small ones develop from the initial fine precipitates.

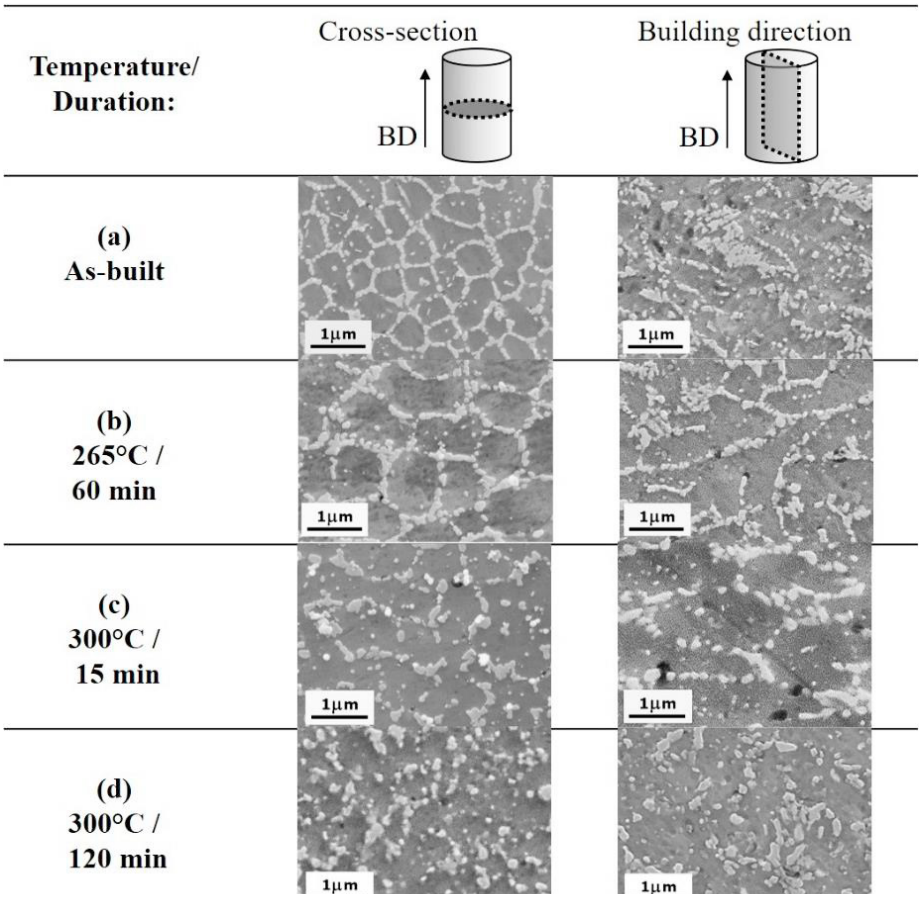

Figure 3: SEM secondary electrons (SEs) micrographs of the L-PBF AlSi10Mg alloy in (a) as-built condition and after stress-relief heat treatments: (b) 265°C for 1 hour; 300°C for (c) 15 min and (d) 120 min.

A further investigation of intermediate stages (i.e., after 30 and 60 min) occurring at 300°C was performed and the results are given in Figure 4. It is possible to notice how the silicon particles are undergoing ruptures reaching a more homogeneous distribution after 2 hours. In particular, 2 hours are necessary to completely break down the silicon networks in the building direction cross-section.

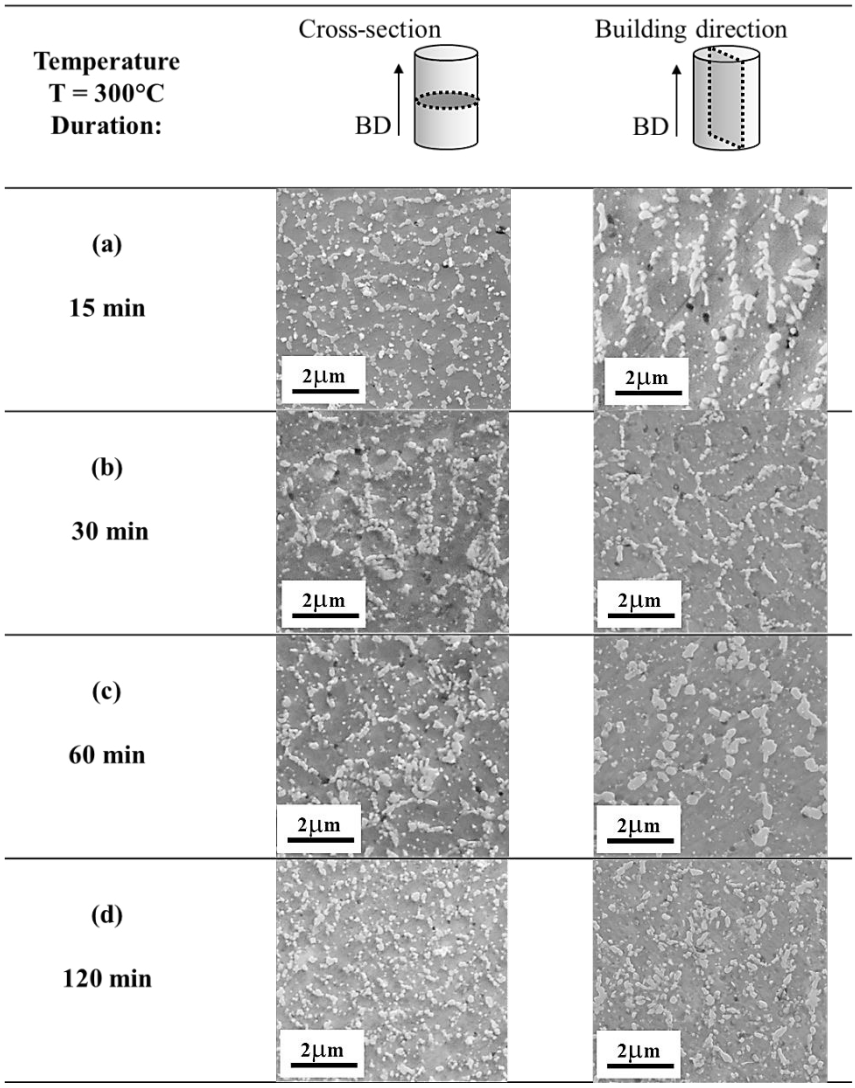

Figure 4: SEM secondary electrons (SEs) micrographs of the L-PBF AlSi10Mg alloy undergoing a heat treatment at 300°C for different durations: (a) 15 min; (b) 30 min; (c) 60 min; (d) 120 min.

In addition to the microstructural analysis, the surface RS were investigated with an X-ray laboratory diffractometer. RS were measured, after cutting the initially fabricated samples in two parts, on the upper half of the specimen (see the geometries in Figure 5). RS along the cylinder height were compared before and after cutting and it was verified that the residual stress state at a distance greater than 10mm from the cut surface was not altered.

A comparison between the as-built condition and two heat treated samples, the one at 265°C for 1 hour and the one at 300°C for 15 min) is shown in Figure 5. The size of the specimens differs by 5 mm, which explains the difference in the number of measured points. The results in Figure 5a show an initial low tensile axial RS component (< 25 MPa) in the as-built condition that is reduced by both the two applied heat treatments. A gradient along the height of the sample, with an increase in tensile RS toward the top, can be observed.

The hoop component varies along the height of the cylinder, changing from compressive, next to the free surface, to tensile, in the middle of the sample (see Figure 5b).

Both heat treatments induce a similar stress relaxation. Even though the axial comment can be considered fully relaxed, the hoop component undergoes a redistribution rather than a full relaxation. Further investigations with a higher penetration depth are foreseen using energy-dispersive X-ray diffraction.

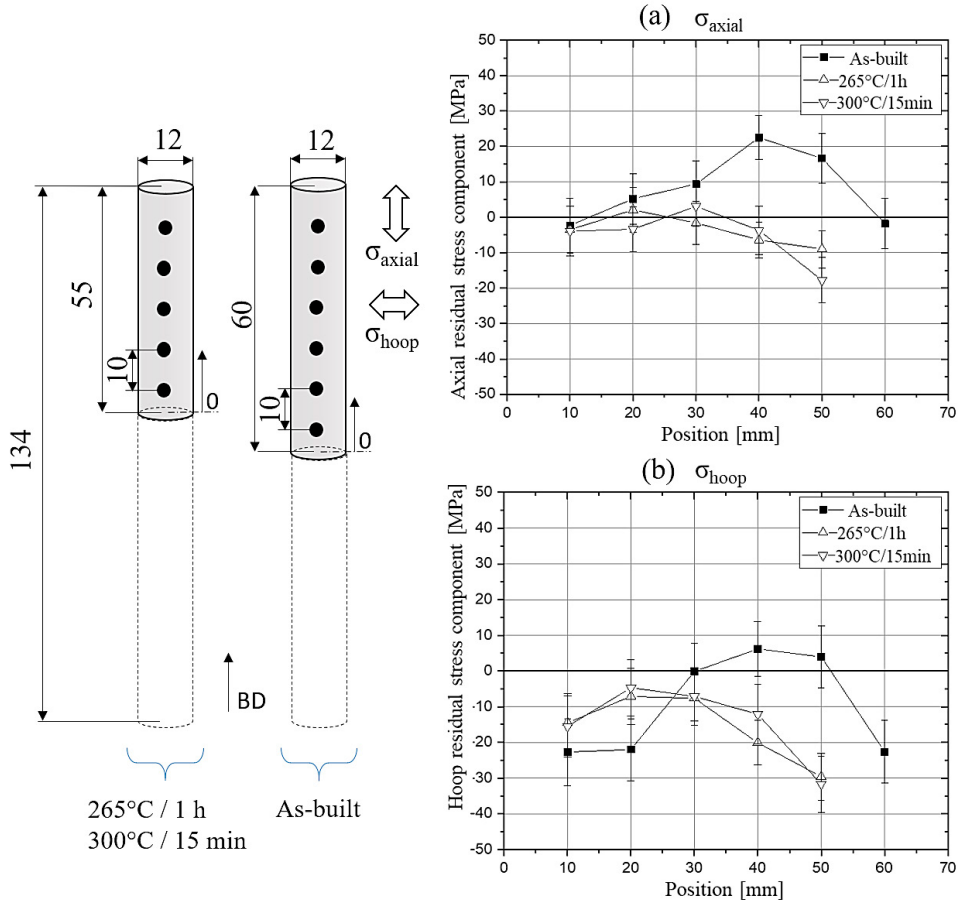

Figure 5: Axial (a) and (hoop) surface RS components along the height of a cylindric sample before and after stress relief heat treatments at 265°C for 1 hour and at 300°C for 15 min. (311) diffraction plane. Penetration depth 10 μm.

4. Conclusion

In this study, the evolution of microstructure and residual stress on a L-PBF AlSi10Mg alloy undergoing different stress relief heat treatments was investigated. Stress relief heat treatments at 265°C and 300°C were compared.

The microstructure is not significantly affected after the 265°C for 1 h heat treatment. A thickening of the Si network, likely due to the precipitation of the supersaturated silicon from the matrix to the silicon boundaries, can be observed. At 300°C for 15 min, the Si network is already broken down into a wide size range of Si particles. During the soaking stage at 300°C, the particles are coarsening (peak of the coarsening is seemingly reached after 1h) and undergoing ruptures reaching a more homogeneous distribution after 2 hours.

In parallel to the microstructure modifications, the surface RS was evaluated. The results show that the performed heat treatments have a comparable effect on the initial RS state. Both heat treatments (at 265°C for 1 h and 300°C for 15 min) are relaxing/redistributing the RS state. Further elucidation of the effects of stress relief schemes on the

RS state will be performed by means of energy-dispersive X-ray diffraction (allowing higher depths, ~300 μm, to be probed).

Evenly distributed spherical silicon particles along with negligible surface tensile or surface compressive RS are expected to be beneficial to the fatigue resistance of the material. To this purpose, two heat treatments will be selected (those two considered to have the best RS and microstructure combination) and tested in the high cycle fatigue regime to evaluate their respective damage tolerance.

Acknowledgements

Deutsches Zentrum für Luft- und Raumfahrt (DLR), Köln, Germany is acknowledged for providing the studied material. Romeo Saliwan Neumann (Bundesanstalt für Materialforschung und -prüfung, Berlin (BAM), Germany) is acknowledged for his expertise and technical assistance during the SEM microstructural investigation. Björn Mieller (Bundesanstalt für Materialforschung und -prüfung, Berlin (BAM), Germany) is acknowledged for performing the heat treatments.

References

L. Thijs, K. Kempen, J.P. Kruth, J. Van Humbeeck, 2013, Fine-structured aluminium products with controllable texture by selective laser melting of pre-alloyed AlSi10Mg powder, Acta Materialia 61, pp. 1809–1819

L.F. Wang, J. Sun, X.L. Yu, Y. Shi, X.G. Zhu, L.Y. Cheng, H.H. Liang, B. Yan, L.J. Guo, 2018, Enhancement in mechanical properties of selectively laser-melted AlSi10Mg aluminum alloys by T6-like heat treatment, Materials Science & Engineering A 734, pp. 299–310

N. Takata, H. Kodaira1, K. Sekizawa1, A. Suzuki, M. Kobashi, 2017, Change in microstructure of selectively laser melted AlSi10Mg alloy with heat treatments, Materials Science & Engineering A 704, pp. 218–228

L. Zhou, A. Mehta, E. Schulz, B. McWilliams, K. Choc, Y. Sohn, 2018, Materials Microstructure, precipitates and hardness of selectively laser melted AlSi10Mg alloy before and after heat treatment, Characterization 143, pp. 5–17

P. Yang, L. A. Deibler, D. R. Bradley, D. K. Stefan, J. D. Carroll, 2018, Microstructure evolution and thermal properties of an additively manufactured, solution treatable AlSi10Mg part, J. Mater. Res. 33

J. Fiocchi, A. Tuissi, C.A. Biffi, 2021, Heat treatment of aluminium alloys produced by laser powder bed fusion: A review, Materials and Design 204

S. Marola, D. Manfredi, G. Fiore, M. G. Poletti, M. Lombardi, P. Fino, L. Battezzati, 2018, A comparison of Selective Laser Melting with bulk rapid solidification of AlSi10Mg alloy, Journal of Alloys and Compounds 742

J. Fiocchi, A. Tuissi, P. Bassani, C.A. Biffi, 2016, Low temperature annealing dedicated to AlSi10Mg selective laser melting products, Journal of Alloys and Compounds 695, pp. 3402-3409

W. Li, S. Li, J. Liu, A. Zhang, Y. Zhou, Q. Wie, C. Yan, Y. Shi, 2016, Effect of heat treatment on AlSi10Mg alloy fabricated by selective laser melting: Microstructure evolution, mechanical properties and fracture mechanism, Materials Science and Engineering: A 663, pp. 116-125

D. Buchbinder, W. Meiners, N. Pirch, K. Wissenbach, J. Schrage, 2014, Investigation on reducing distortion by preheating during manufacture of aluminum components using selective laser melting, Journal of Laser Applications 26